Supplementary Methods and Figures

Modeling Details. Mathematic modeling of transcription dynamics was performed using the Simbiology tool of Matlab. The basic model is depicted in Fig. 7A and parameters values are described here in detail. Transcription dynamics of PhoB-regulated genes depends on two major inputs. One is the phosphorylation kinetics of PhoB and the other is the re-programming of transcription and translation machinery during the Pi starvation stress response, i.e. kinetics of $E\sigma^{70}$ during starvation.

It has been shown that *in vivo* parameters of the PhoBR phosphorylation cycle are dramatically different from parameters determined *in vitro* (1). Therefore, we did not model the PhoB phosphorylation kinetics with limited knowledge of *in vivo* parameters of individual phosphorylation and dephosphorylation reactions. Instead we quantified previous Phos-tag analyses of cellular PhoB~P levels (1, 2) and used the fitted Hill curves as PhoB~P inputs (Fig. 7C). The PhoB~P curve derived from analyses of the constitutive *phoBR* strain RU1616 ([PhoB], 8.2 μM) represents the upper boundary, or the fastest kinetics that a WT strain can achieve if a high level of residual PhoB from prior Pi-starvation remains at the start of the recurrent starvation. The WT curve represents the lower boundary, or the slowest kinetics, with a low initial PhoB level for the recurrent starvation. The parameters for the fitted Hill curves are: maximal PhoB~P level, 3.7 μM (WT) or 4.6 μM (RU1616); half-time, 13 min (WT) or 6.2 min (RU1616); Hill coefficient, 2.0 (WT) or 3.4 (RU1616).

The difference between the two phosphorylation curves is not dramatic because the WT strain can quickly raise the PhoBR levels through autoregulation. The binding constant of PhoB~P to DNA (K_{DNA}) is set at 1 μM, close to the values derived from transcription reporter assays as well as *in vitro* experiments (2). Because the binding affinity of PhoB~P to the

promoter DNA is strong, i.e. the K_{DNA} is low, PhoB~P level exceeds K_{DNA} very shortly after stimulation, thus transcription outputs from the two phosphorylation profiles appear almost indistinguishable (Fig. S5).

It is known that phosphate limitation elicits the stress response (3-5). The stability of stress sigma factor σ^S, the level of ppGpp, the availability of the housekeeping σ^{70} for RNAP binding, and other factors all contribute to the complexity of stress response regulation and re-programming of cells under stress (5, 6). We adopted an extremely simplified model to describe the effects of the stress response on the expression of PhoB-regulated genes. An arbitrary parameter *I* is used to describe the factors that determine the σ^S level and the lump sum inhibitory effects of all factors, such as the anti-σ factor Rsd, ppGpp etc., on the availability of σ^{70} for RNAP binding. The concentrations of σ^S and σ^{70} at a particular time point determine the concentration of $E\sigma^{70}$ and thus the transcription rate. For simplicity, the level of σ^S is chosen to track with [*I*] that has an invariant linear rate of increase (0.0026 a.u./s) upon Pi starvation. The starting level of σ^S varies depending on cellular history and saturates at an arbitrary high level of 24 a.u. (Fig. S3B and S3D). Increase of [*I*] above a threshold Ic, arbitrarily set at 8 a.u., is modeled to decrease the effective concentration of σ^{70} for RNAP binding (Fig. S3B and S3D). The starting concentration of σ^{70} is set at 10 a.u. and the rate of decrease is 0.001 a.u./s.

Different levels of σ^S and σ^{70} lead to the change in $E\sigma^{70}$ level through competition for RNAP. It is assumed that different sigma factors have equal and very strong binding affinities for RNAP so that the concentration of $E\sigma^{70}$ can be described by the equation shown in Materials and Methods based on a simple model (7). This reduces the necessity of including additional affinity parameters for modeling. Including these additional parameters or varying values of the

arbitrarily set parameters does not change the inhibitory nature of the stress response but only alters the dynamics or the relative extent of response homeostasis.

The model is developed to understand the starvation response, or the activation kinetics, not taking into consideration the growth or shut-off of the pathway under Pi-replete conditions. To explain the history-dependent stress response, it is assumed that the concentration of stress factor *I* follows the same growth dilution rule as PhoBR proteins and is modeled as the history-dependent input of the system. A higher initial concentration of *I* will result in an earlier decrease of $E\sigma^{70}$. In other words, a prior stress response will cause an early recurrence of the stress response when cells experience nutrient limitation for the second time. It has been suggested that the phenotypic memory due to protein stability could exist for the σ-associated stress response (8) although there is no detailed characterization of such a memory effect. Our model provides one simplified conceptual explanation for the memory of stress responses. A detailed understanding will need a comprehensive characterization of the dynamics of all factors involved in stress responses.

Figure legends

Fig. S1. Dependence of *phoA-yfp* activation kinetics on growth dilution time. The experiment was performed similarly to the one in Fig. 2 with the same timeline (A). Pre-starved cells were grown in Pi-replete media (1 mM Pi) for indicated growth dilution times followed by re-starvation of Pi. Total fluorescence (B), the increased fluorescence upon stimulation (C), and promoter activities (D) are illustrated with smoothed solid lines. Dashed lines indicate the basal level of fluorescence. Basal levels of fluorescence are different in (B) due to different growth

dilution times and are substracted in (C) to give the increased fluorescence upon re-starvation. Error bars are SDs of 10 individual wells from one microplate assay. Difference between the data here and the one in Fig. 2 may originate from slight differences in growth conditions or stress states. Total fluorescence appeared to converge earlier in this dataset and the rate of fluorescence increase became similar after the fluorescence converged. Despite the difference, pre-starved cells behaved similarly as those in Fig. 2 with cells displaying a relatively high initial promoter activity and an early response repression when growth dilution time is short.

Fig. S2. Attenuation of the response output for pre-starved cultures. (A and B) Reproducibility of reporter output for individual wells from one microplate assay (A) and between independent assays performed in similar growth media (B). The timeline of the experiment is shown at the top. Cells with (*red*) or without (*black*) pre-starvation of Pi were grown in MOPS media containing 50 μM Pi. Approximately 30 min is required for cells to grow and consume the Pi to reach the activation threshold. Individual lines represent data from 8 different wells and the averages are illustrated in (C). (C-E) The increased fluorescence (*top*), total fluorescence (*middle*) and OD (*bottom*) traces for different assays. A fresh preparation of amino acids (AA) mix was added to a final concentration of 40 μg/ml (C) and 4 μg/ml (E) to facilitate the growth. A different preparation of AA mix (different manufacturer lots, long storage at -20°C) was used in a different microplate assay at the concentration of 40 μg/ml for the data in (D). Growth profiles appeared slightly different for the illustrated assays, possibly due to minor differences in AA composition or other growth-related variations. These variations may contribute to different extents of repression by pre-starvation, leading to convergence of fluorescence in some assays but not in others. As shown in the middle panels of (C and D), reporter output differences

between cells with or without pre-starvation were calculated for the end time point (~135 min, D_{end}) as well as the starting point (~24 min, D_{start}) of the recurrent starvation performed in growth media with similar concentrations of nutrients. The ratios of D_{end} over D_{start} from 18 independent microplate assays are plotted as solid circles in (B). A boxplot is shown with the median, the 75 and 25 percentiles together with the whiskers representing SDs. A ratio of 0 indicates a complete convergence of response and the negative value suggests crossing of two curves. If there is no repression or counterbalancing effect, a ratio of 1 with equal differences at the start and end of assay is expected due to the stability of YFP proteins and the extremely slow growth rate under Pi depleted conditions. All pre-starved cells displayed some extent of output attenuation. The average of ratios is 0.24, significantly smaller than 1 with a t-test *p* value smaller than 0.001, suggesting a strong counterbalancing effect.

Fig. S3. Model and simulation of reporter dynamics affected by stress response. (A and B) Model of stress response. Stress response promotes expression of σ^S, which competes with the housekeeping σ^{70} for interactions with RNA polymerase (RNAP). It also increases the level of other factors, e.g. anti-σ factor Rsd and ppGpp, which sequester σ^{70} and effectively inhibit the formation of RNAP-σ^{70} complex, $E\sigma^{70}$. A single arbitrary factor *I* is used to model both effects. Increasing values of [*I*] raise the σ^S level for RNAP competition. The concentration of σ^S is chosen to increase linearly with [*I*] for simplicity and it saturates at a high level (orange line in B). Sequestering of σ^{70} by Rsd or other factors is simplified as concentration reduction of σ^{70} that is capable of binding RNAP. Once [*I*] is above a designated threshold *Ic*, the concentration of RNAP-competent σ^{70} (σ^{70*}) gradually decreases to a minimum level (blue line in B). Concentrations of σ^S and σ^{70*} were used to determine the $E\sigma^{70}$ level with the competition

equation described in Materials and Methods. (C-G) Simulation of pre-starvation and growth dilution. A pre-starvation of 1 h was modeled to increase [*I*] and [Reporter] (C and E). Subsequent growth in Pi-replete media (area shaded in grey) results in growth dilution of [*I*] and [Reporter] to different levels for different lengths of growth time (circles in C and E). These levels were used as initial values of [*I*] and [Reporter] to model output response (D and F). Higher initial concentration of [*I*] results in earlier attainment of the threshold, thus an earlier decrease of σ^{70} (D). This correlates with an earlier decrease of $E\sigma^{70}$ shown in Fig. 7D, leading to an earlier reduction of promoter activity and eventually a convergence of reporter outputs (F). If the stress response is not considered such that the concentration of $E\sigma^{70}$ remains constant, there is no counterbalancing effect on reporter transcription and homeostasis is not reached (G). Protein levels are in arbitrary units (a.u.).

Fig. S4. Dependence of reporter output on stress response kinetics. Different stress response profiles (A and B) are simulated. Linear rates for increase of σ^S are 0.0026 a.u./s (A) and 0.0018 a.u./s (B). Rates of decrease of σ^{70} are 0.001 a.u./s (A) and 0.0007 a.u./s (B). Rates in B were chosen to represent a slower kinetics of stress response than that in A. Dashed lines represent data without any pre-starvation while solid lines indicate data with a growth dilution time of 0.5 h after 1 h of pre-starvation. Vertical dotted lines mark the times that [*I*] reaches the threshold *Ic*. (C and D) Reporter output simulated with stress response profiles above. Reporter levels do not converge within the simulation time (D) when a slow kinetic profile of stress response (B) is used.

Fig. S5. Dependence of reporter output on PhoB~P profiles. The two kinetic PhoB~P profiles from RU1616 and WT, designated as "non-autoregulated" and "autoregulated WT" for *phoBR* expression, represent the boundaries of PhoB~P kinetics for pre-starved WT cells with different growth dilution times. Effects of PhoB~P kinetics on reporter output are simulated at different affinities of PhoB~P to the promoter DNA. Reporter levels are in arbitrary units (a.u.).

References

1. Gao R, Stock AM. 2017. Quantitative kinetic analyses of shutting off a two-component system. MBio 8:e00412-17.
2. Gao R, Stock AM. 2015. Temporal hierarchy of gene expression mediated by transcription factor binding affinity and activation dynamics. MBio 6:e00686-15.
3. Ruiz N, Silhavy TJ. 2003. Constitutive activation of the *Escherichia coli* Pho regulon upregulates *rpoS* translation in an Hfq-dependent fashion. J Bacteriol 185:5984-92.
4. Battesti A, Majdalani N, Gottesman S. 2011. The RpoS-mediated general stress response in *Escherichia coli*. Annu Rev Microbiol 65:189-213.
5. Potrykus K, Cashel M. 2008. (p)ppGpp: still magical? Annu Rev Microbiol 62:35-51.
6. Feklistov A, Sharon BD, Darst SA, Gross CA. 2014. Bacterial sigma factors: a historical, structural, and genomic perspective. Annu Rev Microbiol 68:357-76.
7. Mauri M, Klumpp S. 2014. A model for sigma factor competition in bacterial cells. PLoS Comput Biol 10:e1003845.
8. Lambert G, Kussell E. 2014. Memory and fitness optimization of bacteria under fluctuating environments. PLoS Genet 10:e1004556.

Fig. S1

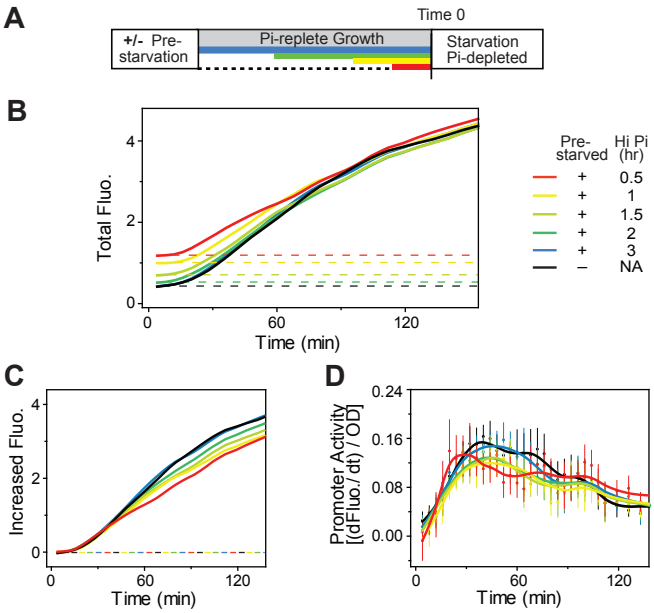

Fig. S1. Dependence of *phoA-yfp* activation kinetics on growth dilution time. The experiment was performed similarly to the one in Fig. 2 with the same timeline (A). Pre-starved cells were grown in Pi-replete media (1 mM Pi) for indicated growth dilution times followed by re-starvation of Pi. Total fluorescence (B), the increased fluorescence upon stimulation (C), and promoter activities (D) are illustrated with smoothed solid lines. Dashed lines indicate the basal level of fluorescence. Basal levels of fluorescence are different in (B) due to different growth dilution times and are substracted in (C) to give the increased fluorescence upon re-starvation. Error bars are SDs of 10 individual wells from one microplate assay. Difference between the data here and the one in Fig. 2 may originate from slight differences in growth conditions or stress states. Total fluorescence appeared to converge earlier in this dataset and the rate of fluorescence increase became similar after the fluorescence converged. Despite the difference, pre-starved cells behaved similarly as those in Fig. 2 with cells displaying a relatively high initial promoter activity and an early response repression when growth dilution time is short.

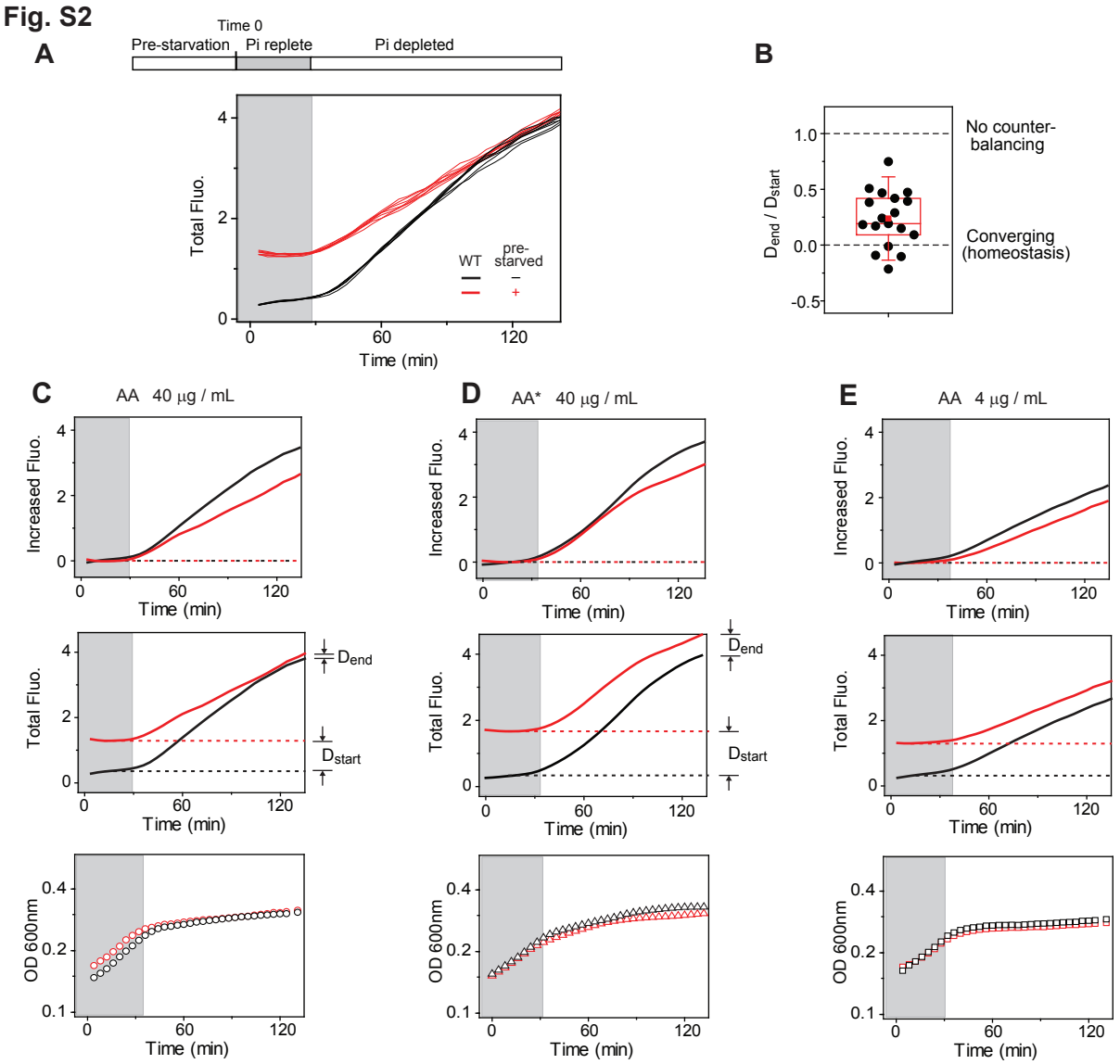

Fig. S2. Attenuation of the response output for pre-starved cultures. (A and B) Reproducibility of reporter output for individual wells from one microplate assay (A) and between independent assays performed in similar growth media (B). The timeline of the experiment is shown at the top. Cells with (*red*) or without (*black*) pre-starvation of Pi were grown in MOPS media containing 50 µM Pi. Approximately 30 min is required for cells to grow and consume the Pi to reach the activation threshold. Individual lines represent data from 8 different wells and the averages are illustrated in (C). (C-E) The increased fluorescence (*top*), total fluorescence (*middle*) and OD (*bottom*) traces for different assays. A fresh preparation of amino acids (AA) mix was added to a final concentration of 40 µg/ml (C) and 4 µg/ml (E) to facilitate the growth. A different preparation of AA mix (different manufacturer lots, long storge at -20°C) was used in a different microplate assay at the concentration of 40 µg/ml for the data in (D). Growth profiles appeared slightly different for the illustrated assays, possibly due to minor differences in AA composition or other growth-related variations. These variations may contribute to different extents of repression by pre-starvation, leading to convergence of fluorescence in some assays but not in others. As shown in the middle panels of (C and D), reporter output differences between cells with or without pre-starvation were calculated for the end time point (~135 min, D_{end}) as well as the starting point (~24 min, D_{start}) of the recurrent starvation performed in growth media with similar concentrations of nutrients. The ratios of D_{end} over D_{start} from 18 independent microplate assays are plotted as solid circles in (B). A boxplot is shown with the median, the 75 and 25 percentiles together with the whiskers representing SDs. A ratio of 0 indicates a complete convergence of response and the negative value suggests crossing of two curves. If there is no repression or counterbalancing effect, a ratio of 1 with equal differences at the start and end of assay is expected due to the stability of YFP proteins and the extremely slow growth rate under Pi depleted conditions. All pre-starved cells displayed some extent of output attenuation. The average of ratios is 0.24, significantly smaller than 1 with a t-test *p* value smaller than 0.001, suggesting a strong counterbalancing effect.

Fig. S3

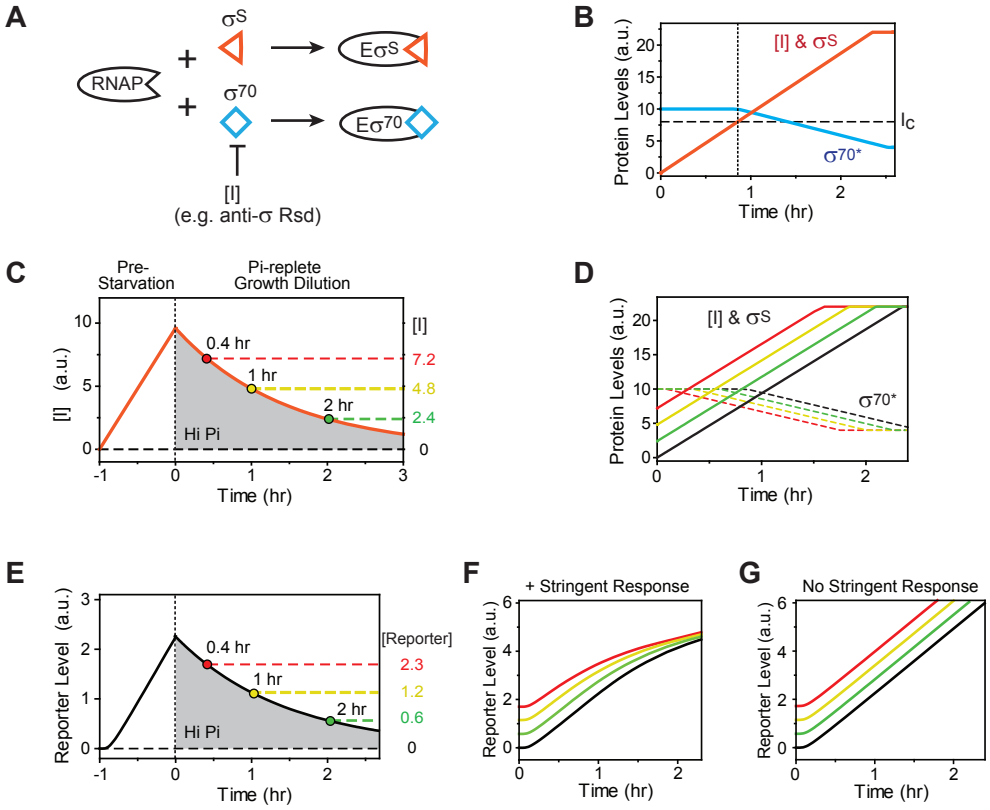

Fig. S3. Model and simulation of reporter dynamics affected by stress response. (A and B) Model of stress response. Stress response promotes expression of σ^S, which competes with the housekeeping σ^{70} for interactions with RNA polymerase (RNAP). It also increases the level of other factors, e.g. anti-σ factor Rsd and ppGpp, which sequester σ^{70} and effectively inhibit the formation of RNAP-σ^{70} complex, $E\sigma^{70}$. A single arbitrary factor *I* is used to model both effects. Increasing values of [*I*] raise the σ^S level for RNAP competition. The concentration of σ^S is chosen to increase linearly with [*I*] for simplicity and it saturates at a high level (orange line in B). Sequestering of σ^{70} by Rsd or other factors is simplified as concentration reduction of σ^{70} that is capable of binding RNAP. Once [*I*] is above a designated threshold *Ic*, the concentration of RNAP-competent σ^{70} (σ^{70*}) gradually decreases to a minimum level (blue line in B). Concentrations of σ^S and σ^{70*} were used to determine the $E\sigma^{70}$ level with the competition equation described in Materials and Methods. (C-G) Simulation of pre-starvation and growth dilution. A pre-starvation of 1 h was modeled to increase [*I*] and [Reporter] (C and E). Subsequent growth in Pi-replete media (area shaded in grey) results in growth dilution of [*I*] and [Reporter] to different levels for different lengths of growth time (circles in C and E). These levels were used as initial values of [*I*] and [Reporter] to model output response (D and F). Higher initial concentration of [*I*] results in earlier attainment of the threshold, thus an earlier decrease of σ^{70} (D). This correlates with an earlier decrease of $E\sigma^{70}$ shown in Fig. 7D, leading to an earlier reduction of promoter activity and eventually a convergence of reporter outputs (F). If the stress response is not considered such that the concentration of $E\sigma^{70}$ remains constant, there is no counterbalancing effect on reporter transcription and homeostasis is not reached (G). Protein levels are in arbitrary units (a.u.).

Fig. S4

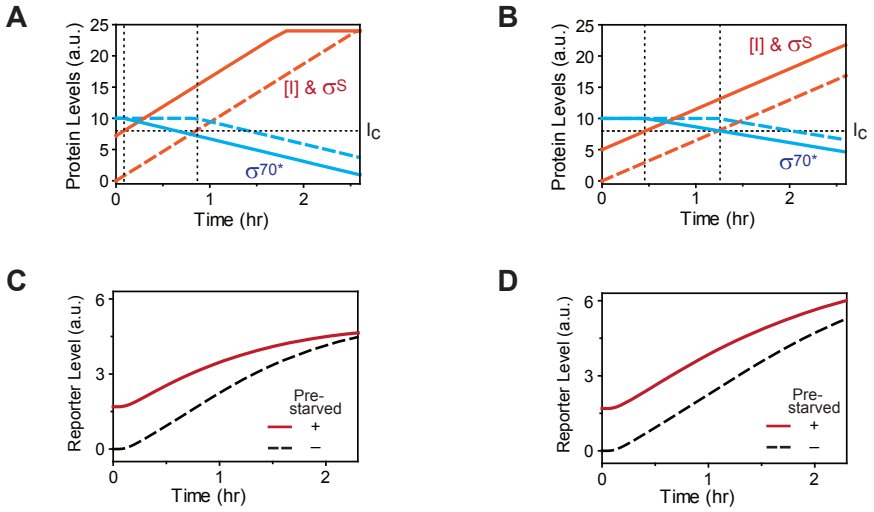

Fig. S4. Dependence of reporter output on stress response kinetics. Different stress response profiles (A and B) are simulated. Linear rates for increase of σ^S are 0.0026 a.u./s (A) and 0.0018 a.u./s (B). Rates of decrease of σ^{70} are 0.001 a.u./s (A) and 0.0007 a.u./s (B). Rates in B were chosen to represent a slower kinetics of stress response than that in A. Dashed lines represent data without any pre-starvation while solid lines indicate data with a growth dilution time of 0.5 h after 1 h of pre-starvation. Vertical dotted lines mark the times that [*I*] reaches the threshold *Ic*. (C and D) Reporter output simulated with stress response profiles above. Reporter levels do not converge within the simulation time (D) when a slow kinetic profile of stress response (B) is used.

Fig. S5

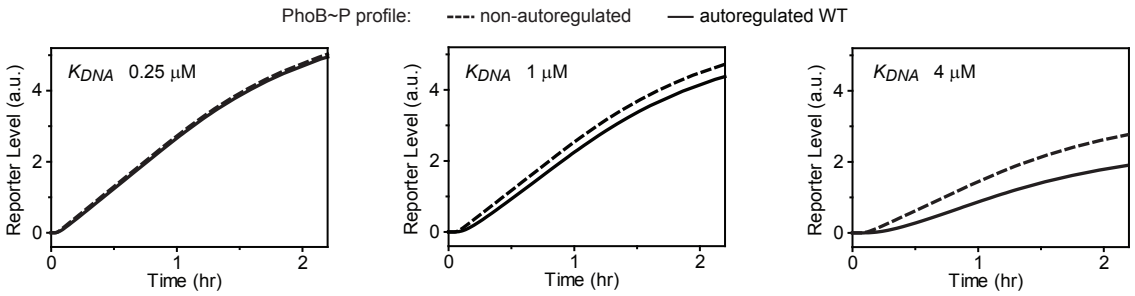

Fig. S5. Dependence of reporter output on PhoB~P profiles. The two kinetic PhoB~P profiles from RU1616 and WT, designated as "non-autoregulated" and "autoregulated WT" for *phoBR* expression, represent the boundaries of PhoB~P kinetics for pre-starved WT cells with different growth dilution times Effects of PhoB~P kinetics on reporter output are simulated at different affinities of PhoB~P to the promoter DNA. Reporter levels are in arbitrary units (a.u.).